Journal of Applied Phycology (2026) 38:113–129
https://doi.org/10.1007/s10811-025-03750-3

RESEARCH

The growth phase of the microalga *Neochloris oleoabundans* influences the production of useful biotechnological molecules and extracellular vesicles

Luna Ardondi[1] · Costanza Baldisserotto[1] · Annalisa Maietti[2] · Barbara Zavan[3] · Simonetta Pancaldi[1]

Received: 18 April 2025 / Revised: 19 November 2025 / Accepted: 23 November 2025 / Published online: 6 January 2026

Abstract
Microalgae are versatile microorganisms that produce bioactive compounds with antioxidant, anti-inflammatory, and antimicrobial properties. *Neochloris oleoabundans* stands out for its adaptability and promising potential in a wide range of biotechnological applications, including the synthesis of high-value metabolites. Among the bioactive molecules of interest, extracellular vesicles (EVs) are gaining increasing attention for their potential in drug delivery and the development of novel therapeutic and healthcare products. The aim of this study is to investigate the microalga and how different growth phases can influence the yield of biologically active molecules with biotechnological relevance. For this reason *N. oleoabundans* (UTEX 1185) was cultivated for an unusually long period of 60 days. Measurements of the PSII maximum quantum yield indicated that the cultures remained in a healthy state even after prolonged cultivation, confirming the robustness of this strain. Biochemical characterisation of both the microalgal biomass and the conditioned medium was performed after 28 and 60 days of cultivation (corresponding to early and late stationary phases, respectively). The results suggest an enhanced production of high-value bioactive compounds during the early stationary phase, which is particularly advantageous given the higher biomass concentration at this stage. EVs were detected in the conditioned medium, with a higher abundance observed after 28 days. Transmission electron microscopy also revealed the presence of vesicles inside the cells, specifically located between the plasma membrane and the cell wall.

Keywords Chlorophyceae · Biotechnology · Growth phases · Bioactive molecules · Extracellular vesicles

Introduction

Microalgae are unicellular photosynthetic microorganisms found in a wide variety of aquatic environments (Thoré et al. 2023). They represent a sustainable resource with numerous benefits; for example, their rapid growth rates, high biomass yields, and the ability to be cultivated on non-arable lands, offer many advantages over traditional crops (Dębowski et al. 2020). Furthermore, their growth requirements can be precisely controlled within photobioreactors, enabling year-round production independent of seasonal fluctuations (Wang et al. 2012). Renowned as 'miniature green factories', they produce a vast array of primary and secondary metabolites including proteins, pigments, and fatty acids (Ohse et al. 2015; Del Mondo et al. 2020; Chini Zittelli et al. 2023). These compounds exhibit a wide spectrum of beneficial properties such as antioxidant (Baldisserotto et al. 2024), anti-inflammatory (Tabarzad et al. 2020), and antimicrobial/antiviral activities (Carbone et al. 2021; Baldisserotto et al. 2023), demonstrating significant potential for niche markets. These microorganisms are remarkably versatile with immense potential to address some of the most pressing challenges of our time, including climate change, food security, sustainable energy production, and human health, such as in the development of new pharmaceuticals and nutraceuticals (Galasso et al. 2019; Ibrahim et al. 2023; Yang et al. 2023). The metabolites produced by microalgae

✉ Simonetta Pancaldi
simonetta.pancaldi@unife.it

[1] Department of Environmental and Prevention Sciences, University of Ferrara, C.So Ercole I d'Este 32, 44121 Ferrara, Italy

[2] Department of Chemical, Pharmaceutical and Agricultural Sciences, University of Ferrara, Via Luigi Borsari 46, 44121 Ferrara, Italy

[3] Department of Medical Sciences, University of Ferrara, Via Fossato Di Mortara 64/B, 44121 Ferrara, Italy

vary significantly depending on the species, the conditions, and the growth phase. Microalgae growth in batch culture typically exhibits six distinct phases: lag, exponential, linear, declining, stationary, and death phases (Mata et al. 2010; Lee et al. 2015). Cells initially undergo a lag phase to adapt to new conditions, followed by exponential growth with rapid division and biomass accumulation. Growth then shifts to a linear phase, limited by light intensity, until nutrient depletion leads to a declining rate (Mata et al. 2010). In the stationary phase, cell division ceases and storage compounds such as starch or lipids accumulate (Chen et al. 2017; Abdullahi et al. 2023), while protein synthesis is reduced due to the nitrate-limited condition (Brown et al. 1993; Paes et al. 2016; Boelen et al. 2017; Syazwina et al. 2022; Abdullahi et al. 2023). Finally, the culture enters the so-called "death phase" characterised by a rapid decline in cell density, attributed to nutrient depletion, pH imbalance, or contamination. As demonstrated in several studies, the metabolic profile of microalgae is not only influenced by growth conditions and species but also exhibits significant variation across different growth phases (Liang et al. 2013; Su et al. 2013; Vello et al. 2018). Beyond biomass production, the spent medium deriving from microalgae cultivation, also called microalgae-conditioned medium (MCM), has emerged as a valuable resource within a circular economy framework; for example, it can be used as recycled water-substrate for microalgae cultivation, thus helping in freshwater saving and reducing production costs (Sabia et al. 2015), or as crop biostimulant (González-Pérez et al. 2022; Braun and Colla 2023; Kim et al. 2023; Žunić et al. 2024). Furthermore, MCM is a promising source of biologically active molecules, such as polysaccharides (Li et al. 2011, 2020) and extracellular vesicles (EVs) (Picciotto et al. 2021, 2022). EVs are particles that are released from cells, delimited by a lipid bilayer, that cannot replicate on their own (Welsh et al. 2024). These vesicles range in size from 30 to 1000 nm and are classified into categories such as exosomes (30–150 nm) and microvesicles (100–1000 nm), depending on their size and how they are formed (Cui et al. 2020; Trentini et al. 2024). EVs carry a variety of cargo, including proteins, lipids, RNA, and other molecules, which they transfer to other cells, thereby influencing numerous biological function (Yáñez-Mó et al. 2015). They are essential in processes like immune modulation, tissue repair, and intracellular communication (Gill et al. 2019; György et al. 2015; Sall and Flaviu 2023). Due to their ability to deliver materials between cells, EVs are becoming a focus for therapeutic innovations, particularly in drug delivery systems and regenerative therapies (Du et al. 2023; Ferroni et al. 2024). Microlgal-derived EVs, for instance, contain bioactive compounds with antioxidant, anti-inflammatory, and healing properties, making them promising candidates for the development of new treatments and health products (Adamo et al. 2021, 2024; Picciotto et al. 2021, 2022). Recently, research has highlighted the potential of plant-derived EVs, especially those derived from microalgae, in therapeutic applications (Picciotto et al. 2022; Adamo et al. 2024). However, little research has been conducted on the growth conditions of microalgae related to EVs production and on assessing the best time to harvest during microalgal growth. Although limited attention has been given to the influence of growth conditions on microalgae-derived EV production and to the identification of the most suitable harvesting stage, recent advances have highlighted the relevance of these factors. In particular, cultivation approaches such as batch-refeed and perfusion cultures have been shown to significantly impact both EV yield and quality (Paganini et al. 2023; Picciotto et al. 2025). These insights emphasize the need to investigate growth-phase-dependent EV production, providing a stronger rationale for optimising cultivation strategies and harvesting time.

Among microalgae of biotechnological interest, *Neochloris oleoabundans* (syn. *Ettlia oleoabundans*) is a unicellular freshwater green species of Chlorophyceae (Chlamydomonadales). Its cells show a spherical shape and typically measure 3–6 µm in diameter; its chloroplast is usually parietal and cup-shaped, enclosing thylakoids and a large pyrenoid, the latter being surrounded by a starch shell (Baldisserotto et al. 2014). *Neochloris oleoabundans* exhibits morphological and physiological plasticity in response to a variety of growth conditions (Safi et al. 2021). The microalga can grow, besides autotrophy, in mixotrophic or heterotrophic conditions (Baldisserotto et al. 2016), in addition freshwater or seawater media can be used for its cultivation (De Jaeger et al. 2018; Rashidi and Trindade 2018; Safi et al. 2021).

Based on these considerations, the aim of the present study was to highlight the possible impact of the early and late stationary growth phases of *N. oleoabundans* on the production of compounds of biotechnological interest, such as proteins, phenolics, polyamines and EVs, obtainable from both microalgae biomass and MCM. It is reasonable to think that early or late stationary growth phases are appropriate times for harvesting, as they are usually correlated with higher biomass yield than lag and exponential phases. However, it is also necessary to verify the biotechnological relevance of the microalgal biomass and its spent medium during the above-mentioned growth phases (Abu Hajar et al. 2017; Altunoz et al. 2017; Li et al. 2020; Barten et al. 2022). Moreover, the morphological and biochemical profiling of *N. oleoabundans* cells during its cultivation, especially at the abovementioned growth phases, was investigated to obtain a more accurate assessment of the microalgal culture and to target its subsequent exploitation. Indeed, at the best of our knowledge, no information is reported on *N. oleoabundans* at the late *vs* early stationary phase of growth. By linking growth phases with the production of both metabolites and

EVs, this work provides insights that can be applied to define optimal harvesting strategies, which in turn may improve the scalability, reproducibility, and sustainability of microalgae-based biotechnological applications.

Materials and methods

Microalgal cultivation and culture conditions

Neochloris oleoabundans UTEX 1185 (syn. *Ettlia oleoabundans*) was obtained from the Culture Collection of Algae at the University of Texas (www.utex.org). The alga was cultured in BG11 medium (for recipe, see Table S1) and maintained in a growth chamber at 24 ± 1 °C, 30 $\mu mol_{photons}$ m^{-2} s^{-1} of photosynthetically active radiation (PAR; white LED LS5020E-NW, Arena Luci Design, Italy) with a light-darkness photoperiod of 16:8 h. CO_2 supply was not provided according to previous studies and static conditions were chosen (only manual shaking two/three times a week) (Baldisserotto et al. 2020). Once the stationary growth phase was reached and a cell density between 20 and 22×10^6 cells mL^{-1} was achieved, cells were inoculated at least in triplicate in 500-mL Erlenmeyer flasks (total volume equal to 350 mL) at a density of $(0.5 \pm 0.1) \times 10^6$ cells mL^{-1} and maintained at the conditions described above. To monitor the growth and the dry microalgal biomass yield increase, 3 flasks were set up and routinely used for measurements. In detail, aliquots of culture were collected from each flask after 0, 3, 7, 10, 14, 21, 28 and 60 days of cultivation for growth measurements. Additionally, at 0, 7, 28 and 60 days of cultivation, microalgal biomass was harvested by centrifugation at 4000 × *g* for 10 min at room temperature (RT). The supernatant was discharged, and the cell pellets were frozen at −20° C until further biochemical analyses including protein and phenolic content (PC) were carried out. For protein analysis, after centrifugation and removal of the supernatant, the biomass was resuspended in 2 mL of washing buffer (2 mM Na_2EDTA in PBS buffer 1×; for 1L of 10×PBS buffer stock solution: 80 g NaCl, 2 g KCl, 14.4 g $Na_2HPO_4.2H_2O$, 2.4 g KH_2PO_4 dissolved in distilled water) and centrifuged at 4000 × *g* for 10 min at RT. Subsequently, supernatant was removed, and the samples were immersed in liquid nitrogen for 1 min, and then stored at −20 °C.

Analyses of *N. oleoabundans* cultures

Growth parameters

Growth of microalgae cultures was assessed through the measurement of cell density (10^6 cells mL^{-1}) and dry biomass yield (g_{DW} mL^{-1}, where DW refers to the dry biomass of microalgae cultures). The cell density was estimated by counting cells with a Thoma counting chamber (HBG, Germany) under the light microscope (Zeiss, model Axiophot, Carl Zeiss, Germany). Growth rates (μ; day^{-1}) were also evaluated, using the following equation (Glenn and Doty 1992):

$$\mu(day^{-1}) = \frac{(\ln N_1 - \ln N_0)}{(t_1 - t_0)}$$

where μ is the growth rate, N_1 is the cell density at time t_1, N_0 is the cell density at time t_0. The time interval (days) is identified as the difference between t_1 and t_0.

The DW was obtained as per Popovich et al. (2012), by adding a set volume of culture (depending on the cell density) to a pre-dried and pre-weighed glass-fiber filter (Whatman GF/C; 1.2 μm pore size); the filter paper containing the microalgae was then rinsed with distilled water (dH_2O) to remove excess salts, dried for 48 h at 60 °C, and weighted to determine the dry biomass yield per unit volume. The pH of the medium was measured using a Jenway mod. 3510 (UK) bench pH-meter. The measurement was conducted after separating the medium from the microalgal biomass by centrifugation at RT at 500 × *g* for 5 min.

Morphological observations of *N. oleoabundans* cells: light and transmission electron microscopy

To assess the morphological traits of the cells, samples were collected routinely. Microscope images were obtained using the light microscope mentioned above and equipped with a VisiCam Pro 20 C digital camera (20 megapixels). Ultrastructure of the cells was also observed after preparation as described in Baldisserotto et al. (2023): culture samples were collected by centrifugation (600 × *g*, 10 min, RT) and prepared as follows: glutaraldehyde (3% *v/v* in phosphate buffer 0.1 M, pH 7.2; 3 h, 4 °C) was used for fixation, and OsO_4 (2% *v/v* in phosphate buffer; 1 h, RT) for post-fixation. Thereafter, cells were dehydrated in acetone series and embedded in Araldite resin. Ultrathin sections were finally stained with lead citrate and uranyl acetate (Baldisserotto et al. 2020). For observations, a Talos L 120 C G2 transmission electron microscope (Thermo Fisher Scientific, USA) was employed, and pictures were taken with a Ceta camera (16 million pixels; Thermo Fisher Scientific), at the Electron Microscopy Center of the University of Ferrara.

PSII maximum quantum yield

During cultivation, aliquots of each biological replicate were harvested by centrifugation at 10,000 × *g* for 5 min at RT. The pellet was resuspended and placed as a single drop on a wet filter paper (Pharma laboratory paper, myCordenons, Italy). After 15 min of dark adaptation, variable fluorescence

measurements were done using a Junior pulse amplitude modulation (PAM) fluorimeter (Walz, Germany) (Ferroni et al. 2018). Samples were exposed to a saturating light pulse (0.6 s) via a fiber optic system, and the basal (F_0) and maximum (F_M) fluorescence levels were recorded to calculate the F_V/F_M ratio ($(F_M - F_0)/F_M$), i.e., the maximum quantum yield of PSII (Kalaji et al. 2014; Ferroni et al. 2018).

Photosynthetic pigments

During cultivation, chlorophyll (Chl) *a* and *b* and total carotenoids (Car) were extracted and quantified as described in (Baldisserotto et al. 2023). Briefly, the samples were centrifuged (10,000 × *g*, 10 min, RT) and 1 mL of pure methanol was added to the microalgal pellet. Subsequently, the samples were placed for 15 min in a thermoblock (uniBLOCHTHERM, LLG Labware) preheated to 80 °C. At the end of the extraction run, the samples were centrifuged (20,000 × *g*), obtaining a clear extract separated from the cell debris. The absorbance was measured spectrophotometrically using a Pharmacia Biotech Ultrospec2000 UV–vis spectrophotometer (1 nm bandwidth; Amersham Biosciences, USA) at 665 nm (Chl*a*), 653 nm (Chl*b*), 470 nm (Car) and 750 nm (background noise). All manipulations were performed under dim green light to avoid photodegradation of pigments. Quantification of pigment concentration in the cuvettes was calculated as follows (Wellburn 1994):

$$\text{Chl}a\left(\mu g\ mL^{-1}\right) = 15.65 \cdot \left(A_{666} - A_{750}\right) - 7.34 \cdot \left(A_{653} - A_{750}\right)$$

$$\text{Chl}b\left(\mu g\ mL^{-1}\right) = 27.05 \cdot \left(A_{653} - A_{750}\right) - 11.21 \cdot \left(A_{666} - A_{750}\right)$$

$$\text{Car}\left(\mu g\ mL^{-1}\right) = \frac{1000 \cdot \left(A_{470} - A_{750}\right) - 2.86\text{Chl}a - 129.2\text{Chl}b}{221}$$

where A_{664}, A_{653}, A_{480}, and A_{750} are the optical densities at 664, 653, 480, and 750 nm, for Chl*a*, Chl*b*, Car, and background noise, respectively.

Data were adjusted considering microalgal volume used for extraction, dilution factors, microalgal DW, and then the results were expressed in micrograms per milligrams of microalgal DW (μg mg_{DW}^{-1}).

Protein extraction and quantification

At 0, 7, 28 and 60 days, total proteins were extracted following the method described by Baldisserotto et al. (2023). To disrupt cells, the frozen sample was subjected to 3 freeze–thaw cycles (2 min in liquid nitrogen followed by 2 min at 80 °C, each) and homogenized with glass beads (0.40–0.60 μm diameter; Sartorius, Germany) by vortexing for 10 min (30 s vortexing, 30 s cooling). After centrifugation at 1500 × *g* for 10 min at RT, the supernatant was collected in a clean Eppendorf tube. The pellet was re-extracted with 500 μL of the same extraction buffer, vortexed for 2 min, and incubated at 60 °C for 15 min to obtain a second extract. These extracts were combined and 30 μL of the final extract were used for quantification using the Lowry assay (Lowry et al. 1951) with slight modification. Bovine serum albumin (BSA; Sigma Chemicals, USA) was used as standard. Protein content was expressed as percentage of microalgal DW (%DW).

Total phenolic compounds extraction and quantification

At 0, 7, 28 and 60 days, a culture volume containing 150×10^6 cells was harvested by centrifugation (10,000 × *g*, 10 min, RT) and the pellet was stored at −20 °C until extraction. Microalgal extract was obtained using a modified version of the methods described in (Haoujar et al. 2019) and (Jerez-Martel et al. 2017). Briefly, 600 μL of pure methanol was added to the pellet. The mixture was then mechanically disrupted by continuous vortexing for 15 min, followed by a 30-min sonication bath, and concluding with 10 min of continuous vortexing. Samples were subsequently centrifuged (10,000 × *g*, 10 min, RT), and the supernatants were collected for quantification of total phenolic compounds (PC). The Folin-Ciocalteu method was used for total phenolics quantification, as described in Haoujar et al. (2019) with minor modifications. Briefly, 100 μL of extract were mixed with 750 μL of Folin-Ciocalteu reagent (Merck, Germany; 1:10 diluted with dH_2O), followed by the addition of 750 μL of sodium carbonate solution (Na_2CO_3, 60 g L^{-1}). After a 5-min incubation at RT, the mixture's absorbance was measured at 725 nm. The total PC of the methanol extracts was expressed as milligrams of coumaric acid equivalents per gram of microalgal DW ($mgE_{Coum.Ac}\ g_{DW}^{-1}$).

Microalgae-conditioned medium (MCM) harvesting and extracellular vesicles isolation

The MCM was collected at time 28 and 60 of cultivation through centrifugation at 300 *g* for 10 min (RT), to separate it from the microalgal biomass. The separated spent medium was then recollected in a clean tube and immediately subjected to further treatment in order to isolate the vesicles, according to the MISEV guidelines (Welsh et al. 2024). The MCM underwent multiple centrifugation steps to remove increasingly dense debris. First, samples were centrifuged at 650 × *g* for 10 min at RT, followed by 3000 × *g* for 30 min, and then at 10,000 × *g* for 1 h, at 4 °C. After centrifugation, the supernatant was passed through 0.22 μm vacuum filtration systems (Sartorius, Germany) to achieve a higher level of purity. The filtrate was centrifuged at 15,000 × *g* for 1 h

at 4 °C. After discarding the resulting pellet, the supernatant underwent a final ultracentrifugation step at 110,000 × *g* for 1.5 h to precipitate the vesicles. The pellet was then resuspended in 1 mL of PBS (Thermo Fisher Scientific) and stored at −80 °C prior to subsequent analyses.

Microalgae-derived EVs quantification and characterization

Nanoparticle Tracking Analysis (NTA) was used to measure vesicles concentration, size and distribution; it utilizes light scattering to estimate particle concentrations in suspension and measures their size based on Brownian motion. This analysis was performed using the NanosightPro instrument (Malvern Panalytical, UK). Microalgae-derived EVs samples were diluted in 1 mL of PBS buffer (Thermo Fisher Scientific, pH 7.4) to optimize the particle concentrations for detection (between 1×10^6 and 1×10^9 particles mL^{-1}). The sample was introduced into a flow chamber at a rate of 3 µL min^{-1}, illuminated by a laser beam and a camera recorded the scattering light. Five sets of 5-min recordings were analysed using the Nanosight software which tracks particle movements in the suspension. The system calculated particle concentration (particles mL^{-1}) and size distribution (nm), considering sample temperature, viscosity, and dilution. Protein content was determined using the Pierce BCA Protein Assay Kit (Thermo Fisher Scientific), following the manufacturer's protocol. Absorbance was measured at 570 nm with a Victor 3 multilabel plate reader (PerkinElmer, Italy). To evaluate the morphology of the microalgae-derived EVs, the vesicles were observed through scanning electron microscopy (SEM). After isolation, microalgae-derived EVs were fixed by resuspension in 1 mL of 2% glutaraldehyde prepared in phosphate buffer. The fixed particles were left to settle by gravity for 1 h on a clean coverslip at RT (25 °C). For SEM analysis, the sample underwent dehydration through sequential washes with ethanol at increasing concentrations (50%, 70%, 80%, 90%, 100%). The coverslip was then mounted on an appropriate support and sputter-coated with gold according to standard procedures. Imaging was carried out under high-vacuum conditions using a Zeiss GeminiSEM 460 (Zeiss, Germany) at the Electron Microscopy Center of the University of Ferrara.

Extraction and determination of polyamines from the MCM

At 28 and 60 days of cultivation, MCM was harvested, separated from the microalgal biomass as previously described, and lyophilised. The extraction process was conducted as described by Sabia et al. (2015) through addition of 300 µL of 4% perchloric acid to 30 mg of accurately weighted freeze-dried sample. The mixture was left on ice for 1 h and subsequently centrifuged at 10,000 × *g* for 15 min. The supernatant, separated from the precipitate, was used for analysis following derivatisation. For the HPLC separation (VP Shimatzu), a Kinetex C18 chromatographic column (Phenomenex), 150 × 4.6 mm, with core–shell spherical particles of 5 µm diameter and thermostatted at 36 °C, was used. The separation was performed with a flow rate of 1 mL min^{-1} in a gradient starting with H_2O 42%, acetonitrile (ACN) 58%; in 7 min H_2O 40% and ACN 60%; in the following 5 min reaching ACN 100%, which was maintained for 4 min, and finally in 4 min returning to the starting conditions. For each run, 10 µL of derivatised sample was injected. The derivatisation reaction followed the Learey et al. (2018) method and was performed directly in the HPLC vial. To 100 µL of sample or standard, 250 µL of saturated sodium carbonate and 250 µL of dansyl chloride (DNS-Cl) were added. After shaking for 1 min, the mixture was left at 40 °C for 45 min. Then, 100 µL of glycine was added, and after 10 min, 500 µL of ACN.

Data analyses

Statistical analysis was performed using R version 4.2.2 (R Core Team 2022). The results of biochemical composition were compared using two-tailed t-test, adopting a significance level of 95% ($\alpha = 0.05$), for two-groups comparisons. In the cases of comparison among more than two groups, a One-way ANOVA test was used ($\alpha = 0.05$). If the assumption of homogeneity of variance and normality were not satisfied, the data were transformed through square root or logarithm. If the ANOVA test indicated $p < 0.05$, a Tukey's post-hoc was conducted. If the data transformation did not fulfil the assumptions, non-parametric Kruskal–Wallis tests was performed. If the test indicated $p < 0.05$, a post-hoc Dunn's test with Bonferroni correction was conducted to identify pairwise differences between groups. Image analysis was performed through ImageJ free software (Schneider et al. 2012).

Results

Growth parameters

Cell density was monitored to determine growth kinetics (Fig. 1A). A typical increasing trend was observed during the first 28 days of cultivation. The exponential phase developed immediately after the inoculation within the first 14 days of cultivation, showing the highest growth rate ($\mu = 0.22$ day^{-1}) compared to those recorded for the following time intervals, i.e. between 14 and 28 days, when the cells continued to divide at a slower rate ($\mu = 0.07$ day^{-1}), and between days 28 and 60, when the lowest growth rate ($\mu = 0.02$ day^{-1}) was measured (ANOVA, $p < 0.05$).

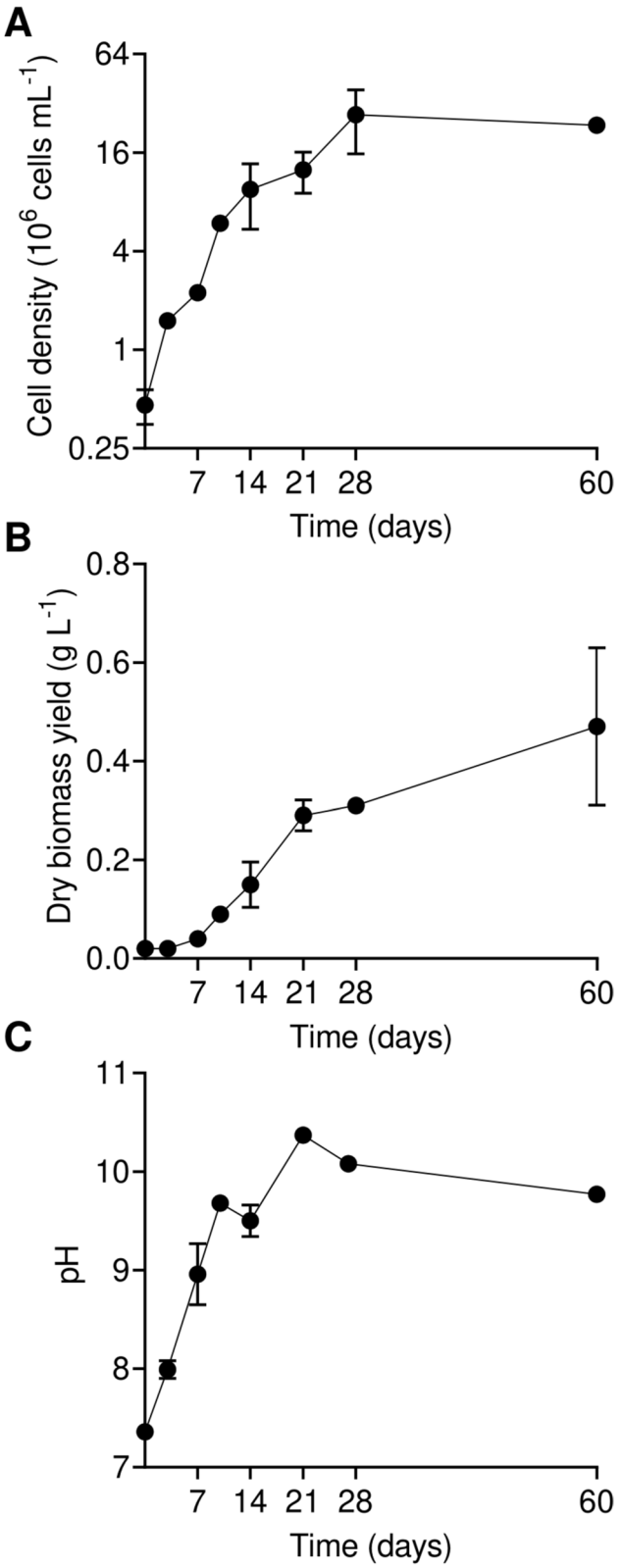

Fig. 1 Growth parameters of *N. oleoabundans* culture over 60 days of cultivation. (**A**) Growth kinetics: cell density values (10^6 cells mL^{-1}), plotted on a base 2 logarithmic scale. (**B**) Dry biomass yield (g_{DW} L^{-1}). (**C**) Trend of pH of the culture medium. Data refer to mean ± standard deviation ($n = 3$)

Throughout the entire cultivation period, the maximum cell density value of 27.2×10^6 cells mL^{-1} was recorded on day 28. By the 60th day, the cell density remained almost unchanged, showing only a slight decrease of about 3×10^6 cells mL^{-1}. Analogously, the dry biomass yield showed an increasing trend for the first 14 days (Fig. 1B): with an initial value of 0.02 g_{DW} L^{-1} and a value of 0.15 g_{DW} L^{-1} on day 14, the data reflected the trend observed for cell density. Subsequently, the values tended to further increase to 0.29 g_{DW} L^{-1} at day 21, then stabilizing to a yield of about 0.31 and 0.36 g_{DW} L^{-1} at days 28 and 60, respectively. The pH of the cultures, as reported in Fig. 1C, showed an immediate and rapid increase from 7.4 to 9.7 during the first 10 days; after a temporary further increase recorded at the 21st day (10.4) of cultivation, in the following days, i.e. from 21 to 60 days, the pH remained quite stable to values around 10.

Observation of microalgae cell morphology

Light microscopy (LM) and transmission electron microscopy (TEM) aimed at improving information on cell morphology and ultrastructure of *N. oleoabundans* at the early (28 days) and late (60 days) stationary growth phase. For LM, an intermediate point was added to check the microalgae cell overall morphology at the exponential phase: in detail, at 7 days of cultivation algae were mostly occupied by a large chloroplast that took almost the entire volume of the cell, and had a cell diameter usually around 4 µm (Fig. 2A and D; Table 1). In contrast, at day 28 cells were quite variable in size: besides cells with an overall appearance similar to that observed for the cells at day 7, smaller and bigger cells were also present (from 3 to 11 µm in diameter) (Fig. 2B and E; Table 1). At 60 days of cultivation, the cells still appeared green, they were homogeneously larger than at both day 7 and 28, but several of them were empty (Fig. 2C and F; Table 1).

TEM images refer to *N. oleoabundans* cells at 28 (Fig. 3A-F) and 60 (Fig. 3G-K) days of cultivation. At the early stationary phase (28 days), cells sometime showed cytoplasmic vacuolisation. Both groups of cells showed the typical main feature of the microalga: one nucleus per cell and a large, cup-shaped chloroplast containing a pyrenoid surrounded by starch and crossed by thylakoids (Fig. 3F and K). Interestingly, many cells from both growth phases showed vesicles of different size between the cell membrane and the cell wall. In particular, in cells from 28 day cultures, vesicles (Fig. 3B) from the top to the bottom measured 142.24 nm, 184.47 nm, 179.34 nm, 342.46 nm, 229.76 nm and 60.20 nm in diameter, respectively (Table 2). Some vesicles were surrounded by a bilayer membrane and measured around 100 nm in diameter (Fig. 3D-E). These vesicles were evidently accumulated in the periplasmic space between membrane and cell wall. The cell wall appeared

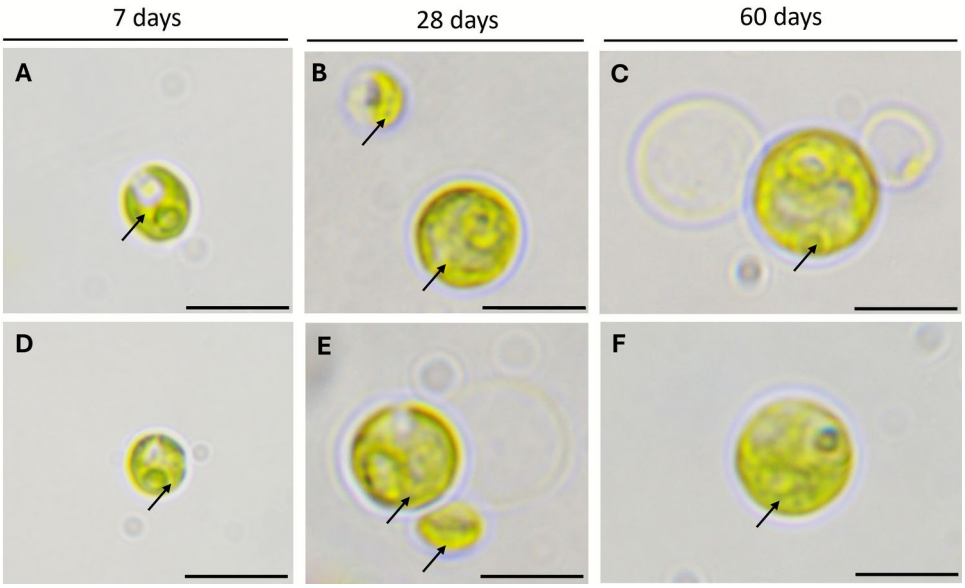

Fig. 2 Light microscopy images of *N. oleoabundans* at day 7 (**A-D**), 28 (**B-E**) and 60 (**C-F**) of cultivation. Arrows, chloroplast. Bars: 5 µm

Table 1 Morphometric measurements of the cell diameter of *N. oleoabundans* at 7, 28 and 60 days of cultivation. Values are mean ± standard deviation ($n = 20$)

Day of cultivation	Mean diameter (µm)	Minimum (µm)	Maximum (µm)
7	4 ± 1^{a}	3	7
28	5 ± 2^{b}	3	11
60	6 ± 0^{b}	5	7

Different superscript letters indicate statistically significant differences between column means (Kruskal–Wallis test, $p < 0.05$)

differently compact in some 60-day-old cells, as shown in Fig. 3I. Indeed, when observing the cell in the image, the cell wall appears less compact on the right and more on the left side (asterisks). The presence of vesicles was also observed in 60 days-old *N. oleoabundans* cells. In Fig. 3H, from the top to the bottom, vesicles pointed by arrows measured 137.38 nm, 124.71 nm, 544.54 nm, 504.68 nm, and 126.01 nm, respectively (Table 2). In Fig. 3J, the vesicles appeared to detach from the membrane. Finally, Fig. 3F and K show an overall image of the samples: in detail, Fig. 3K shows a high concentration of cyst wall residues, that was not observed in the sample at 28 d of cultivation.

Photosynthetic parameters

PSII maximum quantum yield

The F_V/F_M values, starting from 0.597 at time 0, showed a gradual increase which stabilized at around 0.680 between 14 and 28 days of cultivation (Fig. 4). Subsequently, a slight decrease in the general trend was observed, with values of 0.653 at 60 days of cultivation. In general, there was a tendency for F_V/F_M values to increase over time during the first 28 days of cultivation, and then to decrease at the end of experimentation. Statistical analysis indicates that there were significant differences among times ($p < 0.05$).

Photosynthetic pigment content

Photosynthetic pigment concentrations, expressed as µg mg_{DW}^{-1}, are shown in Fig. 5 (A-C). Chl*a* concentration showed a slight, negligible decrease in the first days of cultivation, reaching a minimum around the 3rd-7th day. Subsequently, an increase was observed until a maximum peak was reached on the 21st day, with a value of 64.92 µg mg_{DW}^{-1}. After the peak, a decrease in concentration was recorded, with Chl*a* concentration dropping to values similar to that at the inoculum time (Fig. 5A). Chl*b* followed a trend similar to that of Chl*a*, with an initial decrease, followed by an increase to the maximum peak around the 21st day (25.42 µg mg_{DW}^{-1}), and then a final a decrease that kept stabilized values both at the 28th and the 60th day (14.04 µg mg_{DW}^{-1}) (Fig. 5B). Similarly, carotenoids tended to follow the same trend as chlorophylls content, with the maximum concentration reached on the 21st day (11.25 µg mg_{DW}^{-1}) (Fig. 5C).

Total proteins and phenolics of the microalgal biomass

The highest content of total proteins was present in microalgal biomass after one week from the beginning of the cultivation (day 7; ca 54% DW), with respect to those at 28 and 60 days (41% and 30% DW respectively; Fig. 6A). The values at the early and late stationary phases did not

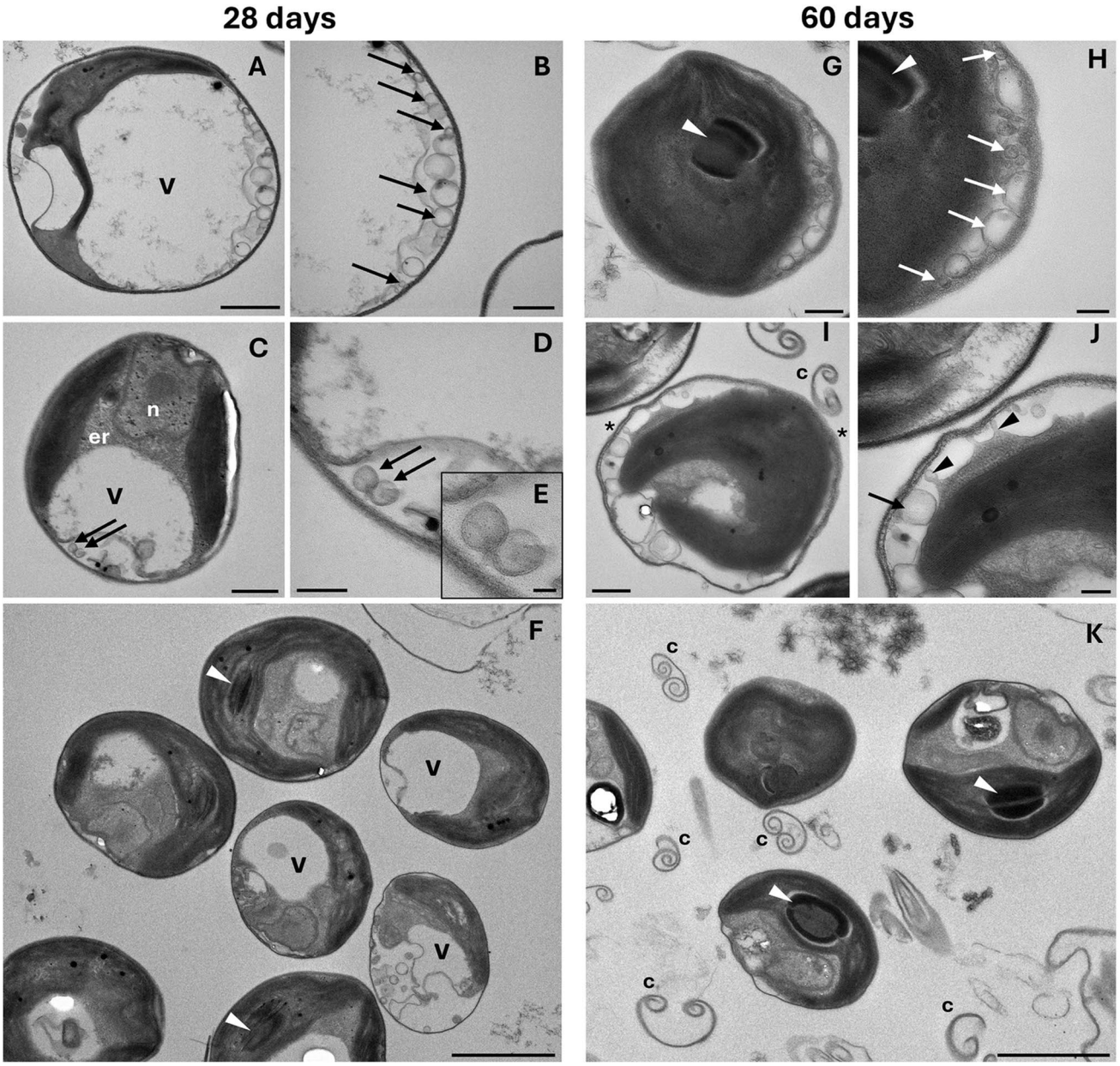

Fig. 3 TEM images of *N. oleoabundans* cells. The two groups of images represent microalgae at 28 days of cultivation (**A-F**) and at 60 days of cultivation (**G-K**). Arrows, vesicles; white arrowhead, pyrenoid; v, vacuolisation; er, endoplasmic reticulum; c, cyst and cell wall residues; n, nucleus; black arrowhead, membrane blebbing; asterisks: cell wall details. Bars: A = 1 µm; B, C, G, I = 500 nm; D, H, J = 200 nm; E = 50 nm; F, K = 2 µm

show significant differences due to the high variability of 28 days samples (*t*-test, $p > 0.05$). Similarly, results on total phenolics (Fig. 6B) showed that the highest concentration was observed in the biomass harvested after 7 days (807.7 $mgE_{Coum.Ac}\ g_{DW}^{-1}$), which was significantly higher than at day 0, 28, and 60 (ANOVA, $p < 0.05$). Moreover, phenolic content at day 28 was also significantly higher than that at day 60 (10.83 *vs* 5.53 $mgE_{Coum.Ac}\ g_{DW}^{-1}$, respectively; $p < 0.05$).

Microalgae-derived extracellular vesicles

In the context of the 28-day microalgae cultures, a comprehensive analysis of microalgae-derived EVs in the microalgae-conditioned medium (MCM) revealed a heterogeneous distribution, as illustrated in Fig. 7A. The maximum particle concentration was observed at 111 nm, reaching approximately 4×10^9 particles mL^{-1}. Most of the isolated vesicles exhibited sizes predominantly ranging from 60 to

Table 2 Dimensions of some representative vesicles highlighted by arrows in the transmission electron images of *N. oleoabundans* at 28 and 60 days of cultivation

Vesicles dimension (diameter, nm)	
28 days	60 days
142.24	137.38
184.47	124.71
179.46	544.54
342.46	504.68
229.76	126.01
60.20	

See vesicles from the top to the bottom in Fig. 3B and H

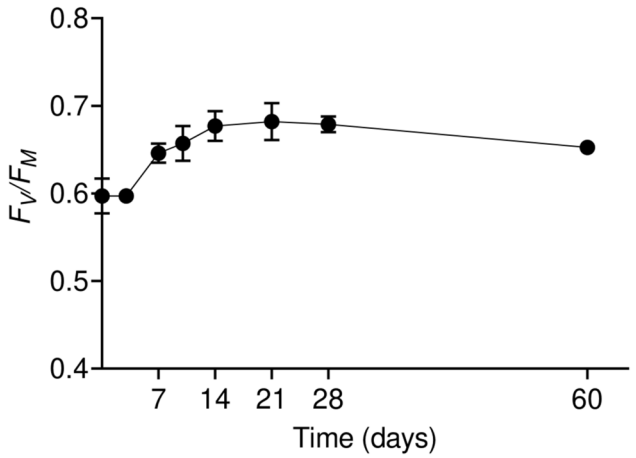

Fig. 4 Time course variations of PSII maximum quantum yield (F_V/F_M ratio) in *N. oleoabundans* cells during the 60 days-long cultivation. Values are mean ± standard deviation ($n = 3$)

150 nm, alongside a notable presence of larger vesicles. The total particle concentration was $8.6 \pm 1.8 \times 10^9$ particles mL^{-1}. Figure 7B illustrates EVs derived from cultures at the 60th day. The maximum particle concentration was detected at 127 nm, reaching 1.4×10^9 particles mL^{-1}. The size distribution in this later stage appeared somewhat less heterogeneous, showing a shift towards larger vesicles compared to those identified in the 28-day cultures. The overall concentration of microalgae-derived EVs was numerically lower, with a value of $7.1 \pm 1 \times 10^9$ particles mL^{-1}, however, the difference in total particle number between the two time points was not statistically significant ($p > 0.05$; $n = 3$). BCA assay revealed protein concentrations of 502 ± 38 and 575 ± 53 µg mL^{-1} in microalgal-derived EVs harvested at 28 and 60 days, respectively, with no significant difference between the two sampling times ($p > 0.05$) (Fig. 7C). SEM images confirmed the presence of EVs in the samples (Fig. 7D, E). The vesicles appeared as spherical structures with sizes consistent with those reported by the NTA analysis.

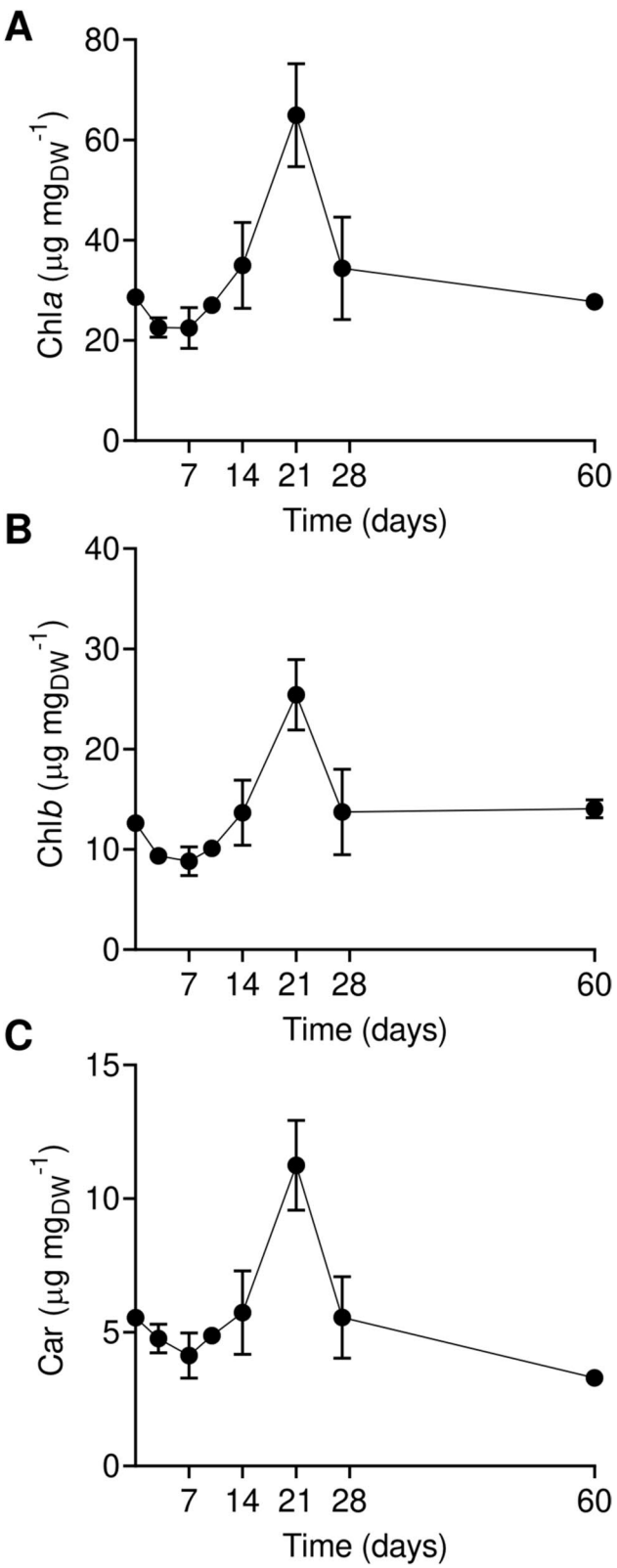

Fig. 5 Time-course variations of photosynthetic pigment concentrations (µg mg_{DW}^{-1}) in *N. oleoabundans* biomass during the 60 days-long cultivation. Graphs show the concentration in µg mg_{DW}^{-1} of (**A**) Chl*a*, (**B**) Chl*b*, and (**C**) Car. Values are mean ± standard deviation ($n = 3$)

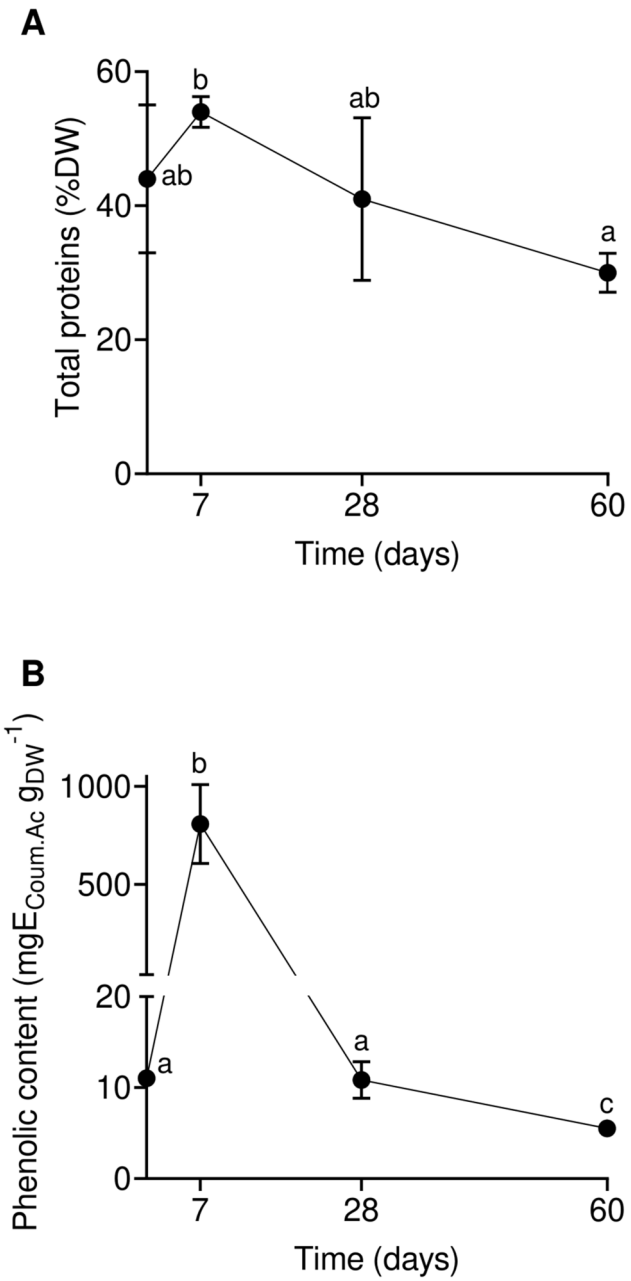

Fig. 6 Time course variations of (**A**) total protein and (**B**) phenolic contents in the microalgal biomass of *N. oleoabundans* at 0, 7, 28 and 60 days of cultivation. Different letters indicate statistically significant groups (ANOVA, $p < 0.05$). Values are mean ± standard deviation ($n = 3$)

Polyamine contents in the microalgae-conditioned medium

The bar chart with results on polyamine (PA) content in the MCM showed the presence of three compounds: spermine, spermidine, and putrescine (Fig. 8). The y-axis represents the concentration of the polyamines in pmol mL^{-1}, while the x-axis displays the different PAs. The data indicate that spermine and spermidine were present in significantly higher concentrations compared to putrescine at both times, 28 and 60 days. The level of spermidine was higher in the 28 days MCM when compared to the 60 days MCM (18.7 *vs* 11.7 pmol mL^{-1}; $p < 0.01$). The levels of spermine appeared to remain relatively stable at both experimental period days, while putrescine was only detected in the MCM collected on day 28 (6.8 pmol mL^{-1}).

Discussion

The morphological and biochemical techniques used in the present work aimed to give more information about the best time, between early and late stationary growth phase (28 and 60 days, respectively), related to the highest concentration of bioactive compounds in the biomass and MCM of autotrophic cultivations of the green microalga *N. oleoabundans*. This is noteworthy considering that *N. oleoabundans* has interesting features and composition, and it has been considered for many biotechnological applications (Valev et al. 2020; Morocho-Jácome et al. 2022; Baldisserotto et al. 2024), in addition to biodiesel production (Baldisserotto et al. 2016).

The measurement of the cell density allowed to identify both the growth kinetics of *N. oleoabundans* and its maximum cell density, which is an important parameter for developing application of microalgae. The overall growth curve showed, after 28 days, a very long stationary phase. Indeed, after 60 days, the culture was still quite stable in cell density and maintained a good physiological condition, as highlighted by the F_V/F_M ratios. It is assumed that, even for microalgae, values of the PSII maximum quantum yield below 0.6 usually refers to a condition of stress and ageing of cultures, while values over 0.6 indicate a good "health" status (Ferroni et al. 2018; Baldisserotto et al. 2022). At the inoculum time cultures were in a quite good state and reached a higher maximum quantum yield of PSII already at the 7th day of cultivation, thus confirming not only that cells were not stressed, but also that the culture conditions were even favourable. The slight decrease in F_V/F_M values at 60 days was probably due to the ageing of the culture.

Cell morphology was observed both by LM and TEM. Measurements of the cell diameter highlighted a value of around 3 µm at the beginning of the experiment and a subsequent, gradual mean increase with time, supporting the more evident increase in dry biomass yield at 28–60 days. However, the main morphological results were derived from TEM analyses, which showed very interesting features of the intracellular and extracellular environments. Besides the most common characteristics of *N. oleoabundans* cells, like the presence of the nucleus and a chloroplast with a large pyrenoid (Baldisserotto et al. 2024), the cells showed

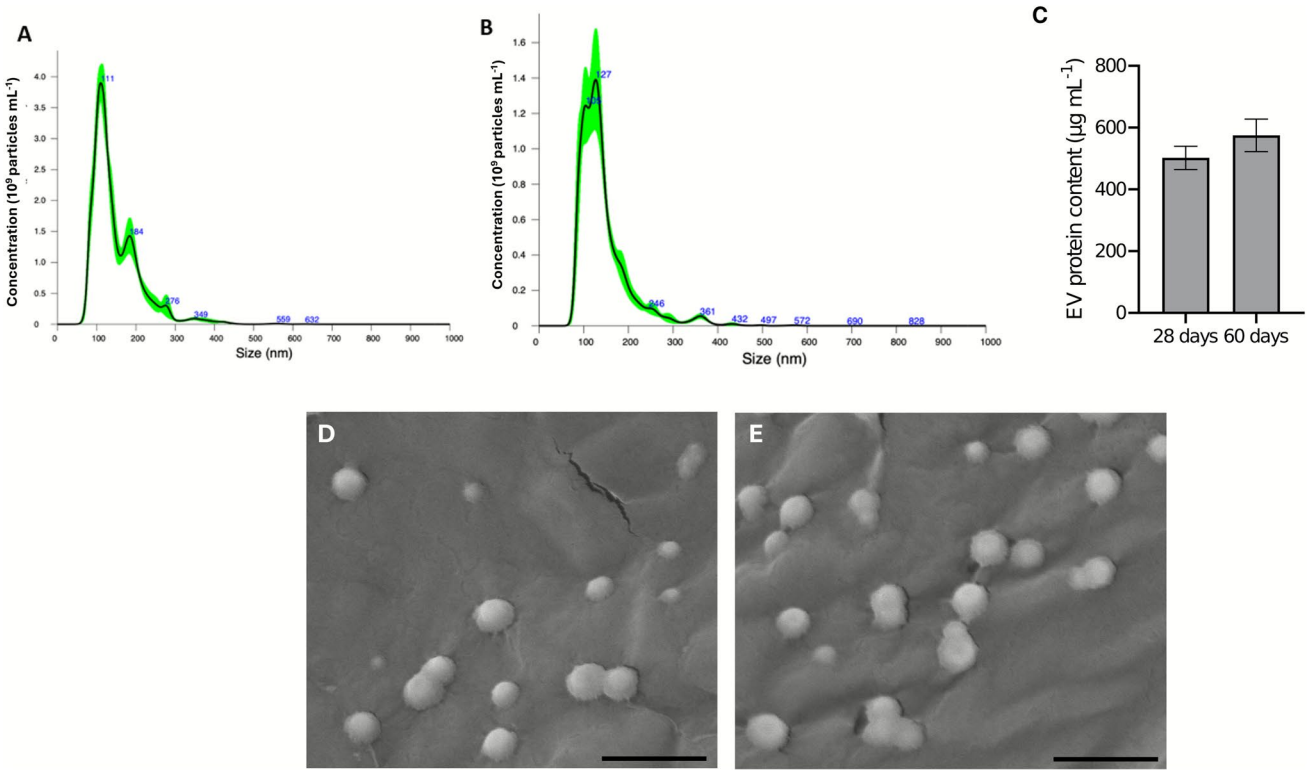

Fig. 7 Analysis of microalgae-derived EVs extracted from the microalgae-conditioned medium (MCM) of *N. oleoabundans* cultures at 28 and 60 days of cultivation. In (**A**) and (**B**), Nanoparticle Tracking Analysis (NTA) representative graphs showing the size distribution and concentration of EVs extracted from MCM at 28 days (**A**) and 60 days (**B**). The MCM of cultures at 28 days exhibit a heterogeneous distribution of vesicles, predominantly ranging from 60 to 150 nm. The 60-day MCM shows a size distribution numerically shifted towards larger vesicles. (**C**) Protein quantification of the microalgae-derived EVs (µg mL^{-1}) at 28 and 60 days. (**D**) and (**E**), Scanning Electron Microscopy (SEM) images of microalgae-derived EVs isolated from the MCM at 28 days of cultivation (**D**) and at 60 days of cultivation (**E**), respectively (MAG, 30.00 KX; WD, 4.4 mm; EHT, 5.00 kV; High Vacuum; bars: 1 µm). In (C), values are mean ± standard deviation ($n = 3$); *t*-test indicates no significant difference between samples ($p > 0.05$)

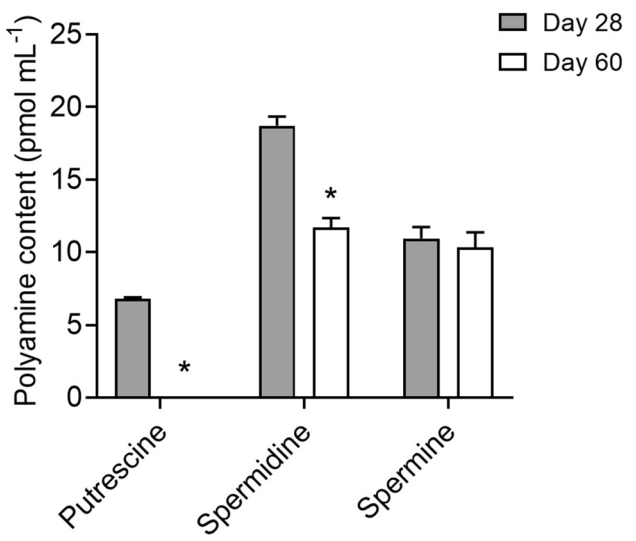

Fig. 8 Polyamine content in the microalgae-conditioned medium of *N. oleoabundans* at 28 and 60 days of cultivation. Values are mean ± standard deviation ($n = 3$). *, significant differences between samples (t-test, $p < 0.05$)

a broad range of vesicles size, both at 28 and 60 days of cultivation. The heterogeneous features of the microalgal cell wall, which appeared more compact on the left side and less compact on the right side of the cell shown in Fig. 3I, could be due to nutrient depletion and/or to the release of cell wall remodelling enzymes from vesicles. The "compact" region reflects the features of the *N. oleoabundans* cell wall previously described by Safi et al. (2021), namely a wall consisting of two rigid layers, which are clearly visible in Fig. 3I (asterisk on the left), and its magnification in Fig. 3J. Concerning the less compact side, it has been demonstrated that the thickness of the *Chlorella* sp. cell wall – which exhibits morphological features similar to *N. oleoabundans* – increases by 70% when cultivated under nitrogen-depleted conditions (Yap et al. 2016; Safi et al. 2021). As for the involvement of cell wall remodelling enzymes, comparable findings have been reported in plants, where vesicles associated with the cell wall were observed, suggesting a role in modifying cell wall texture (De La Canal and Pinedo 2018). This finding could be extended to microalgae, *N.*

oleoabundans included, suggesting that it may be the contents of the vesicles themselves that promote their release through the cell wall, a very strong structure capable of preventing the release of materials, especially large ones (microvesicles, based on their size), to the external environment (Leliaert et al. 2012). Beyond speculation, certain characteristics of the vesicles might provide more precise indications. In both 28- and 60-days samples, the size of the vesicles varied within cells. Exosomes are usually 30 to 150 nm in diameter, while bigger diameters, ranging from 200 to 500 nm, are likely associated with exocyst positive organelles, called EXPO (Regente et al. 2009; Wang et al. 2011). EXPO, described by Wang et al. (2011) and observed in the model plant *Arabidopsis thaliana*, are spherical, double membrane-enclosed structures that fuse with the plasma membrane, releasing a single membrane vesicle outside the plasma membrane and inside the cell wall. As demonstrated in the present study, in addition to vesicles within the cell, EVs have been found in *N. oleoabundans* MCM. Most of these vesicles measured between 60 and 150 nm and thus can be referred as exosomes. In microalgae it is still unknown how vesicle cross the cell wall to be released in the external environment as EVs, and even in plants the mechanism remains unclear. Plant EVs were firstly isolated from extracellular fluid of imbibed sunflower seeds, and they contained defence and cell wall-related proteins (Regente et al. 2009). EVs are flexible and elastic, and they also participate in cell wall remodelling in both plants and fungi (Brown et al. 2015; De La Canal and Pinedo 2018).

This, together with the findings described by Brown et al. (2015), can help explain how EVs could be released in the external medium of thick-walled organisms (Cai et al. 2019) such as *N. oleoabundans*. In the microalga, the variation in size, coupled with a significantly high concentration of microalgae-derived EVs in its MCM, suggests an active and robust release mechanism during the early stationary growth phase (Fig. 7A). Regarding the role of vesicles and EVs in *N. oleoabundans*, the presence of a well-defined lipid bilayer surrounding the vesicles is associated to the essential feature that underpins their functionality and stability (Skotland et al. 2020). Additionally, TEM analysis highlighted the accumulation of low electron-dense vesicles within the space between the plasma membrane and the cell wall (Fig. 3A-D and 3G-J), indicating an intricate interplay of vesicle dynamics within the cellular architecture. This accumulation, along with the observed size distribution, strongly suggests that the cargo of these vesicles could be primarily enriched with biomolecules, including miRNAs and proteins, which are characteristic constituents of plant-derived extracellular vesicles (Trentini et al. 2022, 2024). Such structural and compositional features underscore the potential roles of these vesicles in the mediation of cellular communication and regulatory processes, emphasizing their significance in the physiological responses of the alga to growth-phase transitions and stress factors such as nutrient availability. The lower concentration of EVs observed in 60-day-old samples (Fig. 7B) suggested a reduction in vesicle production or release at the late stationary phase of growth, and it may reflect a response of the algae to prolonged growth. The BCA and SEM analyses of the microalgae-derived-EVs provided complementary information for the characterisation of EVs and confirmed their presence in the MCM. The protein concentration measured by BCA was numerically higher in the EVs isolated from the 60-day-old culture (575 µg mL^{-1}) compared to that from the 28-day-old culture (502 µg mL^{-1}), a difference that was not statistically significant ($p > 0.05$). This trend may be linked to the shift towards larger EVs sizes observed via NTA, suggesting that larger vesicles could potentially contribute to a greater, though variable, protein content. However, this should be regarded only as a hypothesis, which deserves specific further investigation. In addition, SEM imaging supported findings on size of vesicles, also revealing spherical shape and showing intact morphology. Together, these results not only confirm the successful isolation of EVs but also highlight the reliability of combining multiple analytical techniques to assess their abundance, size distribution, and structural integrity. Although this study did not investigate the specific mechanism underlying the release of EVs from microalgae, it is important to consider this aspect. While EVs are produced by all cell types examined to date, including bacteria, plant, fungi, metazoans, and human being (Deatherage and Cookson 2012; Tannetta et al. 2014; Schwechheimer and Kuehn 2015; Budnik et al. 2016), the mechanism of EV release in plant cell and microalgae remain largely unclear. Many mechanisms of EVs release are already well described in other organisms (Beer and Wehman 2017), including exocytosis, where vesicles are released from multivesicular bodies, and ectocytosis, involving direct budding from the plasma membrane (Welsh et al. 2024). In plant cells and microalgae, however, the presence of a rigid cell wall introduces additional complexity. Understanding the mechanisms of EV release in these organisms is particularly important, as it could inform strategies to optimise harvesting processes, maximise yield, and ensure the quality of EVs for biotechnological applications.

With regards to other biochemical features useful for the biotechnological use of *N. oleoabundans* biomass and its MCM, some compounds were evaluated. The photosynthetic pigments in the microalgal biomass were quantified during cultivation: Chls and Car contents showed a similar trend, with a peak at 21 days. Regardless of 21 days, the pigment content remained essentially unchanged between 28 and 60 days, indicating the maintenance of the biomass quality related to them. This is of high biotechnological interest since chlorophyll derivatives are suggested to have

a medicinal application because of their wound-healing and anti-inflammatory properties (Ferruzzi and Blakeslee 2007). Together with pigments, total proteins and phenolics were measured. Proteins, which are the most used microalgae-derived molecules for food and feed applications (Safi et al. 2014) and are usually sold as supplements (Wells et al. 2017), showed the highest concentration at 7 days (54% DW). This result was expected as proteins are usually synthetised during the exponential phase of growth (Amorim et al. 2021), a behaviour confirmed by lower value in the later stages. In any case, a higher protein content was observed in the biomass harvested at 28 days compared to that at 60 days (41 *vs* 30% DW, respectively), although the difference was not statistically significant. Regarding total phenolic content, a peak at 7 days was observed (808 mg g_{DW}^{-1}), then the value tended to decrease, but with higher concentration at 28 than at 60 days of cultivation (10.8 and 5.5 mg g_{DW}^{-1}, respectively). In microalgae, variations in light or nutrient availability strongly influence the phenolic content to avoid cell damage (Goiris et al. 2015). This explains the observed trend, with a high phenolic content after 7 days, probably due to the changes in the environment after inoculum, and a progressive decrease as the culture grew and resources diminished. Besides the meaning of phenolics inside microalgae cells during their cultivation, the comparative result between 28 and 60 days indicates a higher quality of microalgal biomass at the early stationary phase than at the late one. Phenolics are indeed potential substitutes for bioactive agents in pharmaceutical and medicinal sections to promote human health but can also play protective roles against abiotic and biotic stresses (Sun et al. 2023). For example, phenolic compounds are used as food preservatives against fungal and bacterial contaminations (Zamuz et al. 2021; Sun and Shahrajabian 2023). Based on the high applicability of phenolics in several sectors as antioxidants and anti-aging agents, the use of microalgal biomass rich in phenolic compounds, in place of higher plant-derived ones, has been proposed, for example, for the development of cosmeceutical products (Norzagaray-Valenzuela et al. 2017; Gupta et al. 2021).

Finally, polyamines content in the MCM was quantified to better evaluate the presence of bioactive compounds to be valorised in biotechnological applications. MCM from the microalga cultivated in freshwater BG11 contained spermidine, spermine and putrescine, which are the most common polyamines in microalgae (Lin and Lin 2018). The amounts of the above-mentioned polyamines were higher at 28 days than at 60 days of cultivation, and this result is in accordance with what is reported in the literature. Indeed, it is reported that polyamines biosynthesis requires nitrate, and their concentration is reduced under N-limited conditions (Park et al. 2015), a situation that, even if not verified in this work, could have occurred at 60 days. Moreover, it is known that polyamines promote the growth of microalgae, and the increase of putrescine and spermidine during the exponential growth phase of *N. oleoabundans* suggests that these molecules can be closely related to cell division (Treves et al. 2017; Agarwal et al. 2020); this is a possible explanation to the reduction of spermidine and the total absence of putrescine observed at 60 days. Besides in microalgae, polyamines also play important roles in plants, specifically in morphogenesis, growth, embryogenesis, organ development, leaf senescence, and biotic and abiotic stress response (Kusano et al. 2008). For this reason, among others, microalgae have been suggested as biostimulants in agriculture (Mógor et al. 2018). Regarding human health, spermidine and spermine are well recognised polyamines. For example, spermidine is a well-known autophagy inducer that maintains cellular and neuronal homeostasis, thus it is proposed as a therapeutic strategy in neurological disorders (Ghosh et al. 2020); in addition, dietary intake of both spermidine and spermine is recognised to contribute to human health and longevity (Soda et al. 2021). The richness in spermidine and spermine inside the MCM at 28 days represents a further goal in order to exploit the *N. oleoabundans* cultivation for commercial purposes. However, the concentrations measured in this study (6.8, 18.7, and 10.9 pmol mL^{-1} for putrescine, spermidine and spermine, respectively) are relatively low compared to levels reported to induce significant plant growth responses (Mógor et al. 2018). Therefore, the MCM is unlikely to be immediately usable as a commercial biostimulants without an additional concentration or extraction step. Based on Lavandosque and Vischi Winck (2025), the low levels of free polyamines also likely reflect the fact that the culture was not harvested during the optimal growth phase for polyamine accumulation; during the late growth or stationary phase, much of the polyamines may be bound or metabolised, reducing the levels of free compounds available in the medium. Nonetheless, the presence of these compounds indicates that the residual medium could represent a valuable source of bioactive molecules if appropriately processed.

On the whole, the opportunity to combine the exploitation of both the microalgal biomass and the MCM from the same cultivation represents an added value in large-scale microalgal production. Among the various biomolecules investigated within the MCM, EVs represent a novelty, as they have never been observed before in *N. oleoabundans* cultures (cells and spent medium), to the best of the authors' knowledge. Most of the studies present in literature related to EVs from microalgae mainly refer to their bioactivity, toxicity, biocompatibility and potential application, not to the best harvesting time (Adamo et al. 2021, 2024; Picciotto et al. 2022). These studies are fundamental for the further development of therapeutic and related applications, but it is also crucial to know the behaviour and the biology of the

organism producing the vesicles (or other compounds), as well as the best growing conditions, in order to optimally target the production process.

Conclusions

The analysis of *N. oleoabundans* cultures revealed that the 28-day-old biomass exhibits improved biochemical characteristics, particularly in terms of protein (41% DW) and phenolic content (10.83 $mgE_{Coum.Ac}\ g_{DW}^{-1}$), when compared with 60-day-old cultures. At the same cultivation time, the MCM was found to be enriched in microalgae-derived EVs, reaching a concentration of 8.6×10^9 particles mL^{-1}. This production was higher in the early stationary phase than in older cultures.

The co-occurrence of EVs and bioactive metabolites such as polyamines in the 28-day MCM, together with the improved biochemical characteristics of the biomass at the same cultivation stage, opens promising opportunities for the application of both elements in areas such as nutraceutical, agriculture, and biomedicine (Mógor et al. 2018; Ghosh et al. 2020; Soda et al. 2021).

Overall, this study identified 28 days of cultivation as the most suitable time for maximising both metabolite and EVs production, while ensuring the valorisation of both conditioned medium and the microalgal biomass. Future work will focus on the in-depth characterisation of microalgae-derived EVs and intracellular vesicles to unravel their molecular content and biological roles.

Supplementary Information The online version contains supplementary material available at https://doi.org/10.1007/s10811-025-03750-3.

Acknowledgements The Authors are grateful to the Electron Microscopy Center (University of Ferrara) in the persons of Dr. Paola Boldrini and Dr. Edi Simoni for their collaborative efforts in preparing TEM samples and collection of images.

Authors' contributions Conception or design of the work: Luna Ardondi, Simonetta Pancaldi, Costanza Baldisserotto; data collection: Luna Ardondi, Annalisa Maietti; data analysis and interpretation: Luna Ardondi, Costanza Baldisserotto, Barbara Zavan, Annalisa Maietti; drafting the article: Luna Ardondi; critical revision of the article: Simonetta Pancaldi, Costanza Baldisserotto; final approval of the vision to be published: Luna Ardondi, Costanza Baldisserotto, Barbara Zavan, Annalisa Maietti, Simonetta Pancaldi.

Funding Open access funding provided by Università degli Studi di Ferrara within the CRUI-CARE Agreement. This research was funded by the contributions from the University of Ferrara through the Fondo di Ateneo per la Ricerca (FAR).

Data availability The datasets generated and/or analysed during the current study are available from the corresponding author on reasonable request.

Declarations

Competing interests The authors declare no competing interests.

References

Abdullahi ZH, Marselin FN, Khaironizam NIA, Fauzi NF, Wan Maznah WO (2023) Growth stage-related biomass, pigments, and biochemical composition of Stichococcus bacillaris, Synechococcus sp., and Trentepohlia aurea isolated from Gua Tempurung, a cave in Malaysia. Plant Physiol Biochem 197:107633

Abu Hajar HA, Riefler RG, Stuart BJ (2017) Cultivation of the microalga *Neochloris oleoabundans* for biofuels production and other industrial applications (a review). Appl Biochem Microbiol 53:640–653

Adamo G, Fierli D, Romancino D, Picciotto S, Barone M, Aranyos A, Božič D, Morsbach S, Raccosta S, Stanly C, Paganini C, Gai M, Cusimano A, Martorana V, Noto R, Carrotta R, Librizzi F, Randazzo L, Parkes R, Capasso Palmiero U, Rao E, Paterna A, Santonicola P, Iglič A, Corcuera L, Kisslinger A, Di Schiavi E, Liguori G, Landfester K, Kralj-Iglič V, Arosio P, Pocsfalvi G, Touzet N, Manno M, Bongiovanni A (2021) Nanoalgosomes: introducing extracellular vesicles produced by microalgae. J Extracell Vesicles 10:e12081

Adamo G, Santonicola P, Picciotto S, Gargano P, Nicosia A, Longo V, Aloi N, Romancino DP, Paterna A, Rao E, Raccosta S, Noto R, Salamone M, Deidda I, Costa S, Di Sano C, Zampi G, Morsbach S, Landfester K, Colombo P, Wei M, Bergese P, Touzet N, Manno M, Di Schiavi E, Bongiovanni A (2024) Extracellular vesicles from the microalga *Tetraselmis chuii* are biocompatible and exhibit unique bone tropism along with antioxidant and anti-inflammatory properties. Commun Biol 7:941

Agarwal A, Mhatre A, Pandit R, Lali AM (2020) Synergistic biorefinery of *Scenedesmus obliquus* and *Ulva lactuca* in poultry manure towards sustainable bioproduct generation. Bioresour Technol 297:122462

Altunoz M, Pirrotta O, Forti L, Allesina G, Pedrazzi S, Obali O, Tartarini P, Arru L (2017) Combined effects of LED lights and chicken manure on *Neochloris oleoabundans* growth. Bioresour Technol 244:1261–1268

Amorim ML, Soares J, Coimbra JSDR, Leite MO, Albino LFT, Martins MA (2021) Microalgae proteins: production, separation, isolation, quantification, and application in food and feed. Crit Rev Food Sci Nutr 61:1976–2002

Baldisserotto C, Demaria S, Accoto O, Marchesini R, Zanella M, Benetti L, Avolio F, Maglie M, Ferroni L, Pancaldi S (2020) Removal of nitrogen and phosphorus from thickening effluent of an urban wastewater treatment plant by an isolated green microalga. Plants 9:1802

Baldisserotto C, Gentili V, Rizzo R, Di Donna C, Ardondi L, Maietti A, Pancaldi S (2023) Characterization of *Neochloris oleoabundans* under different cultivation modes and first results on bioactivity of its extracts against HCoV-229E virus. Plants 12:26

Baldisserotto C, Gessi S, Ferraretto E, Merighi S, Ardondi L, Giacò P, Ferroni L, Nigro M, Travagli A, Pancaldi S (2024) Cultivation modes affect the morphology, biochemical composition, and antioxidant and anti-inflammatory properties of the green microalga *Neochloris oleoabundans*. Protoplasma 261:1185–1206

Baldisserotto C, Giovanardi M, Ferroni L, Pancaldi S (2014) Growth, morphology and photosynthetic responses of *Neochloris oleoabundans* during cultivation in a mixotrophic brackish medium and subsequent starvation. Acta Physiol Plant 36:461–472

Baldisserotto C, Popovich C, Giovanardi M, Sabia A, Ferroni L, Constenla D, Leonardi P, Pancaldi S (2016) Photosynthetic aspects and lipid profiles in the mixotrophic alga *Neochloris oleoabundans* as useful parameters for biodiesel production. Algal Res 16:255–265

Baldisserotto C, Sabia A, Giovanardi M, Ferroni L, Maglie M, Pancaldi S (2022) Chlorophyta microalgae as dietary protein supplement: a comparative analysis of productivity related to photosynthesis. J Appl Phycol 34:1323–1340

Barten R, Chin-On R, De Vree J, van Beersum E, Wijffels RH, Barbosa MJ, Janssen M (2022) Growth parameter estimation and model simulation for three industrially relevant microalgae: *Picochlorum, Nannochloropsis*, and *Neochloris*. Biotechnol Bioeng 119:1416–1425

Beer KB, Wehman AM (2017) Mechanisms and functions of extracellular vesicle release *in vivo*—what we can learn from flies and worms. Cell Adhes Migr 11:135–150

Boelen P, Van Mastrigt A, Van De Bovenkamp HH, Heeres HJ, Buma AGJ (2017) Growth phase significantly decreases the DHA-to-EPA ratio in marine microalgae. Aquacult Int 25:577–587

Braun JCA, Colla LM (2023) Use of microalgae for the development of biofertilizers and biostimulants. Bioenerg Res 16:289–310

Brown L, Wolf JM, Prados-Rosales R, Casadevall A (2015) Through the wall: extracellular vesicles in Gram-positive bacteria, mycobacteria and fungi. Nat Rev Microbiol 13:620–630

Brown MR, Garland CD, Jeffrey SW, Jameson ID, Leroi JM (1993) The gross and amino acid compositions of batch and semi-continuous cultures of *Isochrysis* sp. (clone T.ISO), *Pavlova lutheri* and *Nannochloropsis oculata*. J Appl Phycol 5:285–296

Budnik V, Ruiz-Cañada C, Wendler F (2016) Extracellular vesicles round off communication in the nervous system. Nat Rev Neurosci 17:160–172

Cai Q, He B, Jin H (2019) A safe ride in extracellular vesicles – small RNA trafficking between plant hosts and pathogens. Curr Opin Plant Biol 52:140–148

Carbone DA, Pellone P, Lubritto C, Ciniglia C (2021) Evaluation of microalgae antiviral activity and their bioactive compounds. Antibiotics 10:746

Chen H, Zheng Y, Zhan J, He C, Wang Q (2017) Comparative metabolic profiling of the lipid-producing green microalga *Chlorella* reveals that nitrogen and carbon metabolic pathways contribute to lipid metabolism. Biotechnol Biofuels 10:153

Chini Zittelli G, Lauceri R, Faraloni C, Silva Benavides AM, Torzillo G (2023) Valuable pigments from microalgae: phycobiliproteins, primary carotenoids, and fucoxanthin. Photochem Photobiol Sci 22:1733–1789

Cui Y, Gao J, He Y, Jiang L (2020) Plant extracellular vesicles. Protoplasma 257:3–12

De Jaeger L, Carreres BM, Springer J, Schaap PJ, Eggink G, Martins Dos Santos VAP, Wijffels RH, Martens DE (2018) *Neochloris oleoabundans* is worth its salt: Transcriptomic analysis under salt and nitrogen stress. PLoS ONE 13:e0194834

De La Canal L, Pinedo M (2018) Extracellular vesicles: a missing component in plant cell wall remodeling. J Exp Bot 69:4655–4658

Deatherage BL, Cookson BT (2012) Membrane vesicle release in bacteria, eukaryotes, and archaea: a conserved yet underappreciated aspect of microbial life. Infect Immun 80:1948–1957

Dębowski M, Zieliński M, Kazimierowicz J, Kujawska N, Talbierz S (2020) Microalgae cultivation technologies as an opportunity for bioenergetic system development—advantages and limitations. Sustainability 12:9980

Del Mondo A, Smerilli A, Sané E, Sansone C, Brunet C (2020) Challenging microalgal vitamins for human health. Microb Cell Fact 19:201

Du S, Guan Y, Xie A, Yao Z, Gao S, Li W, Rao L, Chen X, Chen T (2023) Extracellular vesicles: a rising star for therapeutics and drugdelivery. J Nanobiotechnol 21:231

Ferroni L, Giovanardi M, Poggioli M, Baldisserotto C, Pancaldi S (2018) Enhanced photosynthetic linear electron flow in mixotrophic green microalga *Ettlia oleoabundans* UTEX 1185. Plant Physiol Biochem 130:215–223

Ferroni L, Rubini A, Bargellini P, Tremoli E, Cappucci IP, D'Amora U, Ronca A, Calogero G, Cortellini Panini P, Bettini G, Piccoli C, Rubini G, Sileo L, Cavaleri MP, Lovatti L, Zavan B (2024) Apple vesicles: revolutionary gut microbiota treatment for inflammatory bowel disease. Food Biosci 62:105052

Ferruzzi MG, Blakeslee J (2007) Digestion, absorption, and cancer preventative activity of dietary chlorophyll derivatives. Nutr Res 27:1–12

Galasso C, Gentile A, Orefice I, Ianora A, Bruno A, Noonan DM, Sansone C, Albini A, Brunet C (2019) Microalgal derivatives as potential nutraceutical and food supplements for human health: a focus on cancer prevention and interception. Nutrients 11:1226

Ghosh I, Sankhe R, Mudgal J, Arora D, Nampoothiri M (2020) Spermidine, an autophagy inducer, as a therapeutic strategy in neurological disorders. Neuropeptides 83:102083

Gill S, Catchpole R, Forterre P (2019) Extracellular membrane vesicles in the three domains of life and beyond. FEMS Microbiol Rev 43:273–303

Glenn EP, Doty MS (1992) Water motion affects the growth rates of *Kappaphycus alvarezii* and related red seaweeds. Aquaculture 108:233–246

Goiris K, Van Colen W, Wilches I, León-Tamariz F, De Cooman L, Muylaert K (2015) Impact of nutrient stress on antioxidant production in three species of microalgae. Algal Res 7:51–57

González-Pérez BK, Rivas-Castillo AM, Valdez-Calderón A, Gayosso-Morales MA (2022) Microalgae as biostimulants: a new approach in agriculture. World J Microbiol Biotechnol 38:4

Gupta P, Trivedi U, Rajput M, Oza T, Chauhan J, Sanghvi G (2021) Antiaging and skin lightening microbial products. In: Singh SP, Upadhyay SK (eds) Bioprospecting of microorganism-based industrial molecules. Wiley & Sons, Chichester, pp 47–76

György B, Hung ME, Breakefield XO, Leonard JN (2015) Therapeutic applications of extracellular vesicles: clinical promise and open-questions. Annu Rev Pharmacol Toxicol 55:439–464

Haoujar I, Cacciola F, Abrini J, Mangraviti D, Giuffrida D, Oulad El Majdoub Y, Kounnoun A, Miceli N, Fernanda Taviano M, Mondello L, Rigano F, Skali Senhaji N (2019) The contribution of carotenoids, phenolic compounds, and flavonoids to the antioxidative properties of marine microalgae isolated from Mediterranean Morocco. Molecules 24:4037

Ibrahim TNBT, Feisal NAS, Kamaludin NH, Cheah WY, How V, Bhatnagar A, Ma Z, Show PL (2023) Biological active metabolites from microalgae for healthcare and pharmaceutical industries: a comprehensive review. Bioresour Technol 372:128661

Jerez-Martel I, García-Poza S, Rodríguez-Martel G, Rico M, Alfonso-Olivares C, Gómez-Pinchetti JL (2017) Phenolic profile and antioxidant activity of crude extracts from microalgae and cyanobacteria strains. J Food Qual 2017:1–8

Kalaji HM, Schansker G, Ladle RJ, Goltsev V, Bosa K, Allakhverdiev SI, Brestic M, Bussotti F, Calatayud A, Dąbrowski P, Elsheery NI, Ferroni L, Guidi L, Hogewoning SW, Jajoo A, Misra AN, Nebauer SG, Pancaldi S, Penella C, Poli D, Pollastrini M, Romanowska-Duda ZB, Rutkowska B, Serôdio J, Suresh K, Szulc W, Tambussi E, Yanniccari M, Zivcak M (2014) Frequently asked questions about in vivo chlorophyll fluorescence: practical issues. Photosynth Res 122:121–158

Kholssi R, Ramos PV, Marks EAN, Montero O, Rad C (2021) Biotechnological uses of microalgae: a review on the state of the art and challenges for the circular economy. Biocatal Agric Biotechnol 36:587–621

Kim Y-N, Choi JH, Kim SY, Yoon YE, Choe H, Lee KA, Kantharaj V, Kim MJ, Lee YB (2023) Biostimulatory effects of *Chlorella fusca* CHK0059 on plant growth and fruit quality of strawberry. Plants 12:4132

Kusano T, Berberich T, Tateda C, Takahashi Y (2008) Polyamines: essential factors for growth and survival. Planta 228:367–381

Lavandosque LL, Vischi Winck F (2025) Polyamine-mediated growth regulation in microalgae: integrating redox balance and amino acids pathway into metabolic engineering. SynBio 3:8

Learey JJ, Crawford-Clark S, Bowen BJ, Barrow CJ, Adcock JL (2018) Detection of biogenic amines in pet food ingredients by RP-HPLC with automated dansyl chloride derivatization. J Sep Sci 41:4430–4436

Lee E, Jalalizadeh M, Zhang Q (2015) Growth kinetic models for microalgae cultivation: a review. Algal Res 12:497–512

Leliaert F, Smith DR, Moreau H, Herron MD, Verbruggen H, Delwiche CF, De Clerck O (2012) Phylogeny and molecular evolution of the green algae. Crit Rev Plant Sci 31:1–46

Li H, Li Z, Xiong S, Zhang H, Li N, Zhou S, Liu Y, Huang Z (2011) Pilot-scale isolation of bioactive extracellular polymeric substances from cell-free media of mass microalgal cultures using tangential-flow ultrafiltration. Process Biochem 46:1104–1109

Li Y, Wang C, Liu H, Su J, Lan CQ, Zhong M, Hu X (2020) Production, isolation and bioactive estimation of extracellular polysaccharides of green microalga *Neochloris oleoabundans*. Algal Res 48:101883

Liang C, Cao S, Zhang X, Zhu B, Su Z, Xu D, Guang X, Ye N (2013) De novo sequencing and global transcriptome analysis of *Nannochloropsis* sp. (Eustigmatophyceae) following nitrogen starvation. Bioenerg Res 6:494–505

Lin H-Y, Lin H-J (2018) Polyamines in microalgae: something borrowed, something new. Mar Drugs 17:1

Lowry OH, Rosebrough NJ, Farr AL, Randall RJ (1951) Protein measurement with the Folin phenol reagent. J Biol Chem 193:265–275

Mata TM, Martins AA, Caetano NS (2010) Microalgae for biodiesel production and other applications: a review. Renew Sustain Energy Rev 14:217–232

Mógor ÁF, Ördög V, Lima GPP, Molnár Z, Mógor G (2018) Biostimulant properties of cyanobacterial hydrolysate related to polyamines. J Appl Phycol 30:453–460

Morocho-Jácome AL, Santos BBD, Carvalho JCMD, Almeida TSD, Rijo P, Velasco MVR, Rosado C, Baby AR (2022) Microalgae as a sustainable, natural-oriented and vegan dermocosmetic bioactive ingredient: the case of *Neochloris oleoabundans*. Cosmetics 9:9

Norzagaray-Valenzuela CD, Valdez-Ortiz A, Shelton LM, Jiménez-Edeza M, Rivera-López J, Valdez-Flores MA, Germán-Báez LJ (2017) Residual biomasses and protein hydrolysates of three green microalgae species exhibit antioxidant and anti-aging activity. J Appl Phycol 29:189–198

Ohse S, Bianchini Derner R, Ávila Ozório R, Gordo Corrêa R, Badiale-Furlong E, Cunha PCR (2015) Lipid content and fatty acid profiles in ten species of microalgae. Idesia 33:93–101

Olabi AG, Shehata N, Sayed ET, Rodriguez C, Anyanwu RC, Russell C, Abdelkareem MA (2023) Role of microalgae in achieving sustainable development goals and circular economy. Sci Total Environ 854:158689

Paes CRPS, Faria GR, Tinoco NAB et al (2016) Growth, nutrient uptake and chemical composition of *Chlorella* sp. and *Nannochloropsis oculata* under nitrogen starvation. Lat Am J Aquat Res 44:275–292

Paganini C, Boyce H, Libort G, Arosio P (2023) High-yield production of extracellular vesicle subpopulations with constant quality using batch-refeed cultures. Adv Healthc Mater 12:e2202232

Park J, Wang H, Gargouri M, Deshpande RR, Skepper JN, Holguin FO, Juergens MT, Shachar-Hill Y, Hicks LM, Gang DR (2015) The response of *Chlamydomonas reinhardtii* to nitrogen deprivation: a systems biology analysis. Plant J 81:611–624

Peng L, Zhang Z, Cheng P, Wang Z, Lan CQ (2016) Cultivation of *Neochloris oleoabundans* in bubble column photobioreactor with or without localized deoxygenation. Bioresour Technol 206:255–263

Picciotto S, Barone ME, Fierli D, Aranyos A, Adamo G, BoŽič D, Romancino DP, Stanly C, Parkes R, Morsbach S, Raccosta S, Paganini C, Cusimano A, Martorana V, Noto R, Carrotta R, Librizzi F, Capasso Palmiero U, Santonicola P, Iglič A, Gai M, Corcuera L, Kisslinger A, Di Schiavi E, Landfester K, Liguori GL, Kralj-Iglič V, Arosio P, Pocsfalvi G, Manno M, Touzet N, Bongiovanni A (2021) Isolation of extracellular vesicles from microalgae: towards the production of sustainable and natural nanocarriers of bioactive compounds. Biomater Sci 9:2917–2930

Picciotto S, Santonicola P, Paterna A, Rao E, Raccosta S, Romancino DP, Noto R, Touzet N, Manno M, Di Schiavi E, Bongiovanni A, Adamo G (2022) Extracellular vesicles from microalgae: uptake studies in human cells and *Caenorhabditis elegans*. Front Bioeng Biotechnol 10:830189

Picciotto S, Belmonte D, Gargano P, Adamo G, Paterna A, Rao E, Conlon T, Raccosta S, Romancino DP, Smeraldi G, Salamone M, Touzet N, Manno M, Bongiovanni A (2025) Optimizing sustainable production of high-quality microalgae-derived extracellular vesicles through batch-refeed perfusion cultivation. J Biotechnol 406:236–243

Popovich CA, Damiani C, Constenla D, Martínez AM, Freije H, Giovanardi M, Pancaldi S, Leonardi PI (2012) *Neochloris oleoabundans* grown in enriched natural seawater for biodiesel feedstock: evaluation of its growth and biochemical composition. Bioresour Technol 114:287–293

R Core Team (2022) R: A language and environment for statistical computing. R Foundation for Statistical Computing, Wien, Austria

Rashidi B, Trindade LM (2018) Detailed biochemical and morphologic characteristics of the green microalga *Neochloris oleoabundans* cell wall. Algal Res 35:152–159

Regente M, Corti-Monzón G, Maldonado AM, Pinedo M, Jorrín J, de la Canal L (2009) Vesicular fractions of sunflower apoplastic fluids are associated with potential exosome marker proteins. FEBS Lett 583:3363–3366

Sabia A, Baldisserotto C, Biondi S, Marchesini R, Tedeschi P, Maietti A, Giovanardi M, Ferroni L, Pancaldi S (2015) Re-cultivation of *Neochloris oleoabundans* in exhausted autotrophic and mixotrophic media: the potential role of polyamines and free fatty acids. Appl Microbiol Biotechnol 99:10597–10609

Safi C, Pollio A, Olivieri G (2021) *Neochloris oleoabundans* from nature to industry: a comprehensive review. Rev Environ Sci Biotechnol 20:943–958

Safi C, Zebib B, Merah O, Pontalier PY, Vaca-Garcia C (2014) Morphology, composition, production, processing and applications of *Chlorella vulgaris*: a review. Renew Sustain Energy Rev 35:265–278

Sall IM, Flaviu TA (2023) Plant and mammalian-derived extracellular vesicles: a new therapeutic approach for the future. Front Bioeng Biotechnol 11:1215650

Schneider C, Rasband W, Eliceiri K (2012) NIH image to ImageJ: 25 years of image analysis. Nat Methods 9:671–675

Schwechheimer C, Kuehn MJ (2015) Outer-membrane vesicles from gram-negative bacteria: biogenesis and functions. Nat Rev Microbiol 13:605–619

Skotland T, Sagini K, Sandvig K, Llorente A (2020) An emerging focus on lipids in extracellular vesicles. Adv Drug Deliv Rev 159:308–321

Soda K, Uemura T, Sanayama H, Igarashi K, Fukui T (2021) Polyamine-rich diet elevates blood spermine levels and inhibits pro-inflammatory status: an interventional study. Med Sci 9:22

Su X, Xu J, Yan X, Zhao P, Chen J, Zhou C, Zhao F, Li S (2013) Lipidomic changes during different growth stages of *Nitzschia closterium* f. *minutissima*. Metabolomics 9:300–310

Sun W, Shahrajabian MH (2023) Therapeutic potential of phenolic compounds in medicinal plants—natural health products for human health. Molecules 28:1845

Sun Y, Zhang J, Xu J, Cao J, Li Y (2023) The effects of different LED lights on the main nutritional compositions of *Isochrysis zhanjiangensis*. Fishes 8:124

Syazwina SS, Basri EM, Maznah WOW (2022) Biomass, proximate biochemical composition and fatty acid profiles associated with the growth phase of *Chlorella salina* Butcher and *Isochrysis maritima* Billard and Gayral isolated from the coastal waters of Penang, Malaysia. Aquacult Int 30:899–918

Tabarzad M, Atabaki V, Hosseinabadi T (2020) Anti-inflammatory activity of bioactive compounds from microalgae and cyanobacteria by focusing on the mechanisms of action. Mol Biol Rep 47:6193–6205

Tannetta D, Dragovic R, Alyahyaei Z, Southcombe J (2014) Extracellular vesicles and reproduction—promotion of successful pregnancy. Cell Mol Immunol 11:548–563

Thoré ESJ, Muylaert K, Bertram MG, Brodin T (2023) Microalgae. Curr Biol 33:R91–R95

Trentini M, Zanolla I, Tiengo E, Zanotti F, Sommella E, Merciai F, Campiglia P, Licastro D, Degasperi M, Lovatti L, Bonora M, Danese A, Pinton P, Zavan B (2024) Link between organic nanovescicles from vegetable kingdom and human cell physiology: intracellular calcium signalling. J Nanobiotechnol 22:68

Trentini M, Zanotti F, Tiengo E, Camponogara F, Degasperi M, Licastro D, Lovatti L, Zavan B (2022) An apple a day keeps the doctor away: Potential role of miRNA 146 on macrophages treated with exosomes derived from apples. Biomedicines 10:415

Treves H, Murik O, Kedem I, Eisenstadt D, Meir S, Rogachev I, Szymanski J, Keren N, Orf I, Tiburcio AF, Alcázar R, Aharoni A, Kopka J, Kaplan A (2017) Metabolic flexibility underpins growth capabilities of the fastest growing alga. Curr Biol 27:2559-2567

Valev D, Silva Santos H, Tyystjärvi E (2020) Stable wastewater treatment with *Neochloris oleoabundans* in a tubular photobioreactor. J Appl Phycol 32:399–410

Vello V, Umashankar S, Phang S-M, Chu W-L, Lim P-E, Majid NA, Liew K-E, Swarup S, Chew F-T (2018) Metabolomic profiles of tropical *Chlorella* and *Parachlorella* species in response to physiological changes during exponential and stationary growth phase. Algal Res 35:61–75

Wang B, Lan CQ, Horsman M (2012) Closed photobioreactors for production of microalgal biomasses. Biotechnol Adv 30:904–912

Wang J, Ding Y, Wang J, Hillmer S, Miao Y, Lo SW, Wang X, Robinson DG, Jiang L (2011) EXPO, an exocyst-positive organelle distinct from multivesicular endosomes and autophagosomes, mediates cytosol to cell wall exocytosis in *Arabidopsis* and tobacco cells. Plant Cell 22:4009–4030

Wellburn AR (1994) The spectral determination of chlorophylls *a* and *b*, as well as total carotenoids, using various solvents with spectrophotometers of different resolution. J Plant Physiol 144:307–313

Wells ML, Potin P, Craigie JS, Raven JA, Merchant SS, Helliwell KE, Smith AG, Camire ME, Brawley SH (2017) Algae as nutritional and functional food sources: revisiting our understanding. J Appl Phycol 29:949–982

Welsh JA, Goberdhan DCI, O'Driscoll L, Buzas EI, Blenkiron C, Bussolati B, Cai H, Di Vizio D, Driedonks TAP, Erdbrügger U, Falcon-Perez JM, Fu Q-L, Hill AF, Lenassi M, Lim SK, Mahoney MG, Mohanty S, Möller A, Nieuwland R et al (2024) Minimal information for studies of extracellular vesicles (MISEV2023): from basic to advanced approaches. J Extracell Vesicles 13:e12404

Yáñez-Mó M, Siljander PRM, Andreu Z, Bedina Zavec A, Borràs FE, Buzas EI, Buzas K, Casal E, Cappello F, Carvalho J, Colás E, Cordeiro-da Silva A, Fais S, Falcon-Perez JM, Ghobrial IM, Giebel B, Gimona M, Graner M, Gursel I et al (2015) Biological properties of extracellular vesicles and their physiological functions. J Extracell Vesicles 4:27066

Yang Y, Hassan SHA, Awasthi MK et al (2023) The recent progress on the bioactive compounds from algal biomass for human health applications. Food Biosci 51:102267

Yap BHJ, Crawford SA, Dagastine RR, Scales PJ, Martin GJO (2016) Nitrogen deprivation of microalgae: effect on cell size, cell wall thickness, cell strength, and resistance to mechanical disruption. J Ind Microbiol Biotechnol 43:1671–1680

Zamuz S, Munekata PES, Dzuvor CKO, Zhang W, Sant'Ana AS, Lorenzo JM (2021) The role of phenolic compounds against *Listeria monocytogenes* in food. A review. Trends Food Sci Technol 110:385–392

Žunić V, Hajnal-Jafari T, Stamenov D, Djurić S, Tomić J, Pešaković M, Grohar MC, Stampar F, Veberic R, Hudina M, Jakopic J (2024) Application of microalgae-based biostimulants in sustainable strawberry production. J Appl Phycol 36:1219–1231